Desalination and Water Treatment
www.deswater.com

doi: 10.5004/dwt.2018.21947

108 (2018) 311–321
March

Enhancement of photocatalytic degradation of organic dyes using ZnO decorated on reduced graphene oxide (rGO)

Yean Ling Pang[a,*], Su Fang Tee[a], Steven Lim[a], Ahmad Zuhairi Abdullah[b], Hwai Chyuan Ong[c], Chien-Hou Wu[d], Woon Chan Chong[a,e], Abdul Wahab Mohammad[e], Ebrahim Mahmoudi[e]

[a]*Department of Chemical Engineering, Lee Kong Chian Faculty of Engineering and Science, Universiti Tunku Abdul Rahman, 43000 Kajang, Selangor, Malaysia, Tel. +603-9086 0288; Fax: +603-9019 8868; emails: pangyl@utar.edu.my (Y.L. Pang), sufang2512@1utar.my (S.F. Tee), stevenlim@utar.edu.my (S. Lim), chongwchan@utar.edu.my (W.C. Chong)*
[b]*School of Chemical Engineering, Universiti Sains Malaysia, Nibong Tebal, 14300 Penang, Malaysia, email: chzuhairi@usm.my*
[c]*Department of Mechanical Engineering, Faculty of Engineering, University of Malaya, 50603 Kuala Lumpur, Malaysia, email: onghc@um.edu.my*
[d]*Department of Biomedical Engineering and Environmental Sciences, College of Nuclear Science, National Tsing Hua University, Hsinchu 30013, Taiwan, email: chwu@mx.nthu.edu.tw*
[e]*Department of Chemical and Process Engineering, Faculty of Engineering and Built Environment, Universiti Kebangsaan Malaysia, 43600 Bangi, Selangor, Malaysia, emails: drawm@ukm.edu.my (A.W. Mohammad), ebi.dream@gmail.com (E. Mahmoudi)*

Received 2 August 2017; Accepted 24 January 2018

ABSTRACT

Reduced graphene oxide (rGO) with excellent electron capturing ability could be coupled with semiconductor photocatalyst to prevent the recombination problem of photogenerated hole–electron pairs encountered by pure zinc oxide (ZnO) while simultaneously promote the photocatalytic activity. In this study, rGO decorated with ZnO (ZnO/rGO) photocatalyst was synthesized for the photocatalytic degradation of rhodamine B, congo red and methyl orange in water. The ZnO and ZnO/rGO photocatalysts were characterized by using field emission scanning microscopy-energy dispersive X-ray analysis and X-ray powder diffraction, and Fourier transformed infrared spectroscopic analyses. The morphology and elemental results showed that both catalysts were in spherical shape and free from impurities. It was found that the average particle size of ZnO/rGO was smaller than that of pure ZnO which indicated that ZnO decorated on graphene sheet would decrease the particle size. Congo red showed the highest degradation efficiency and it was attributed to the rapid break down of its azo bond (–N=N–) and aromatic rings by hydroxyl radicals. It was found that 97.96% degradation could be achieved in 1 h under optimum conditions which were at 10 mg/L of initial congo red concentration, 2 g/L of ZnO/rGO catalyst dosage and a solution pH of 7. The spent ZnO/rGO exhibited high catalytic activity of 96.67% at optimum conditions indicating its high stability to act as a photocatalyst. The photocatalytic degradation of congo red satisfactorily fitted a pseudo-first-order reaction kinetic. Besides, the removal of chemical oxygen demand for congo red after 1 h of photocatalytic degradation was nearly 100%.

Keywords: ZnO/rGO; Characteristics; Photocatalytic degradation; Congo red; Reaction kinetic

* Corresponding author.

1. Introduction

There are about one million tonnes of synthetic dyes produced across the globe annually [1]. It is estimated that 280,000 tonnes of textile dyes are being discharged in industrial effluents annually [2]. Several conventional treatment methods such as adsorption, coagulation, flocculation, biodegradation, membrane separations and ion exchange have been developed to remove the organic dyes in wastewater [3]. However, these methods do not destroy organic compounds completely, economically unfeasible and generate secondary pollutants which could accelerate ecosystem deterioration. In addition, they are inefficient to treat various types of dyes and large volume of sewage.

In contrast to conventional methods, advanced oxidation processes especially heterogeneous photocatalytic processes may achieve complete degradation of aromatic organic dyes owning to its high efficiency, good reproducibility and low toxicity [3]. Photocatalytic processes are low or non-residue generation technologies that degrade recalcitrant structures by utilizing short lifetime radical species which possess high oxidation power. Photochemical reaction could be accelerated with the presence of photocatalysts, that is, semiconductor materials and UV radiation. It is performed by three oxidizing agents, that is, hydroxyl radicals ($^{\bullet}OH$), superoxide ions ($^{\bullet}O_2^-$) and positive charge holes (h^+) [4,5]. When semiconductors are excited by the photons from UV radiation that is equal to or higher than their energy bandgap, electrons are promoted from valence bands (VB) to conduction bands (CB). Therefore, holes are created in the VB. The separated electrons and holes will travel to the surface of the semiconductor materials to reduce oxygen and oxidize water molecules adsorbed to form superoxide ions and hydroxyl radicals, respectively. The generated oxidants will subsequently degrade the organic pollutants into carbon dioxide, water and other inorganic compounds.

Among all the photocatalysts, zinc oxide (ZnO) is a nanomaterial that possesses similar optical and photocatalytic properties such as titanium dioxide (TiO_2) and capable to absorb larger solar spectrum compared with TiO_2 [6]. ZnO is commonly used in electronic, optical and photonic devices due to its low cost, high catalytic activity, biocompatibility nature, good electro-optical properties, high electron mobility and high electrochemical stability [7,8]. ZnO can also perform as a photocatalyst to degrade dyes, pesticides, trace metals, organic compounds and inactive bacteria or virus in wastewater treatment. The main drawbacks of ZnO photocatalyst are related to its relatively low photocatalytic activity due to low surface area and high recombination rate of photogenerated electron–hole pairs that restrict its potential applications. Recently, various research investigations have been conducted on the combination of the photocatalysts with metals, narrow band gap energy of semiconductors and carbonaceous materials in order to enhance the photocatalytic activity. Theoretically, the transfer efficiency of photoinduced electron in ZnO can be enhanced by incorporating good electron acceptor such as graphene oxide (GO) [6]. GO is a two-dimensional (2D) network of hexagonal structured sp^2-hybridized carbon atoms that possesses unique properties such as extremely high electron mobility of 2×10^5 cm^2/V s, large specific surface area, high electron conductivity for storing and transporting electrons and excellent chemical stability [5,9]. Meanwhile, reduced graphene oxide (rGO) with reduced number of functionalities and higher capturing electrons abilities is expected to contribute to the suppressing of charge recombination [10]. However, pure rGO shows extremely weak photocatalytic activity with high adsorption capacity [11]. Photocatalytic performance can be significantly improved if rGO is used as a proper substrate to support inorganic semiconductor catalysts.

Hence, the synergetic interaction between rGO and ZnO may yield enhanced catalytic performance due to the excellent individual properties of rGO and ZnO [12]. The incorporation of rGO into semiconductor could minimize the recombination rate of electrons and holes prevent aggregation of the nanoparticles and produce a higher surface area for adsorption of organic dyes [13]. Semiconductor component often acts as the light harvester. Meanwhile, the role of rGO is to perform as a conductive media for accepting and transporting photogenerated electrons. Under UV light radiation with sufficient energy, photogenerated electrons might migrate from the wide band gap semiconductor, that is, ZnO to a 'zero band gap' semiconductor, that is, rGO. The formation of heterojunction results in more efficient interelectron transfer between two materials, which prolongs the lifetime of electron–hole [14]. Besides, rGO could enhance the adsorption capacity and extend the light absorption range of the rGO-based composite photocatalyst. The possibility of rGO to act as a photosensitizer for semiconductor under visible light irradiation could also worth for investigation [13].

Although several papers had reported the preparation of ZnO/rGO samples using sol–gel, hydrothermal, hydrolysis and chemical etching methods which involved higher concentration of rGO for their photocatalytic application [7,11,15,16], the complicated multistep processes had limited their practical applications. Hence, a simplified impregnation method at ambient temperature was employed to synthesize ZnO/rGO composites in this study, which requires less fabrication procedures and no heating process involved to dissolve the precursors in the medium as compared with previous studies. In addition, current development of photocatalytic process behaviour of organic dyes is not well documented. Thus, the novelty of this study lies in the synergic application of ZnO in combination with rGO at low concentration and developed via a single step impregnation of zinc nitrate followed by calcination method under nitrogen flow. This study is aimed to develop a simpler, cost-effective, time-efficient and environmentally friendly for the preparation of ZnO/rGO composite and evaluates their photocatalytic activity towards degradation of organic dyes.

2. Experimental

2.1. Materials

All the reagents used were of analytical grade. Zinc nitrate hexahydrate ($Zn(NO_3)\cdot 6H_2O$ from SYSTERM Chemicals Company (Malaysia) and 99.0% sodium hydroxide (NaOH) supplied by Merck Chemicals Company (Malaysia) were used as the starting materials to synthesize ZnO. 95.0% ethanol (C_2H_6O) from Chemsol Solutions Company (Malaysia) was used as a solvent during the synthesis of photocatalyst.

Meanwhile, GO was synthesized using a modified Hummer's method [17]. Rhodamine B ($C_{28}H_{31}ClN_2O_3$), congo red ($C_{32}H_{22}N_6Na_2O_6S_2$) and methyl orange ($C_{14}H_{14}N_3NaO_3S$) were purchased from Sigma-Aldrich Company (Malaysia) as the model dye compounds to be degraded by the synthesized photocatalysts. The solution pH was adjusted using 0.1 M of hydrochloric acid (HCl) and 0.1 M of NaOH.

2.2. Preparation of ZnO and ZnO/rGO photocatalysts

GO was synthesized using graphite powder according to Hummers method. The detail procedures for preparing the GO catalyst had been described in the literature [17,18]. In order to prepare ZnO/rGO catalyst via a simplified impregnation method, 80 mL of ethanol was mixed with 5.0 wt% of GO in a sonicator for 10 min. After that, 4.0 g of zinc nitrate hexahydrate was added into the mixture and stirred continuously for 1 h. Then, 1.0 g of NaOH and 20 mL of ethanol were added and continuously stirred for another 3 h. The synthesized mixture was dried in an oven at 80°C for 1 d. The dried powder was then calcined at 400°C for 2 h using a horizontal tubular furnace (Lenton, UK, LTF 12/100/940/3216CC) under nitrogen gas flow to obtain ZnO/rGO.

2.3. Sample characterizations

Surface morphologies and elemental composition of the synthesized ZnO and ZnO/rGO were observed using a JEOL JSM-6701F field emission scanning electron microscope equipped with an energy dispersive X-ray system. X-ray diffractometer (Shidmazu XRD-6000) was used to study the crystalline phase and crystallite size of the synthesized photocatalysts under normal atmospheric conditions. The diffractometer was operated at 40 kV and 30 mA with Cu K_α wavelength (λ) of 0.154 nm (1.54 Å). The diffraction patterns of the photocatalysts were scanned at 2θ ranging from 10° to 80° at a scanning speed of 2°/min. Fourier transformed infrared (FTIR) spectrometer (Nicolet iS10) was used to examine the chemical functional groups of the photocatalysts. The FTIR spectra were recorded between the wavenumber of 4,000–400 cm^{-1}.

2.4. Photocatalytic degradation of organic dyes and analysis of liquid samples

A hot plate was used to continuously stir the dye solution with photocatalyst during the photocatalytic process under the presence of UV light. The UV radiation source with a wavelength of 302 nm was achieved by means of a UVP 2UV™ benchtop transilluminator. Experimental conditions used throughout the study were fixed at an initial dye concentration of 10 mg/L and a photocatalyst concentration of 2 g/L unless otherwise specified. The concentrations of the dye solutions were detected at their maximum absorbances, that is, 555, 500 and 505 nm for rhodamine B, congo red and methyl orange, respectively, using a JENWAY 6320D UV-Vis spectrophotometer. In addition, HACH DR3900 spectrophotometer was used to measure the chemical oxygen demand (COD) content of the liquid sample. For each photocatalytic degradation test of organic dye, three experimental runs were conducted to obtain an average value of the degradation efficiency.

2.5. Reusability study

In order to investigate the reusability of photocatalyst, 10 mg/L of congo red was first degraded by 2.0 g/L of ZnO/rGO at a solution pH of 7 for a duration of 1 h. The spent ZnO/rGO was then filtered from the treated solution, washed with distilled water and dried. Then, the spent photocatalysts were used for the degradation of congo red under the same conditions.

2.6. Kinetic study

The kinetic reaction order of photocatalytic degradation using ZnO/rGO was also investigated. The kinetic models for pseudo-zero-order, pseudo-first-order and pseudo-second-order can be described as:

$$\text{Pseudo-zero-order kinetic: } C_t = C_0 - k_0 t \quad (1)$$

$$\text{Pseudo-first-order kinetic: } \ln C_t = \ln C_0 - k_1 \quad (2)$$

$$\text{Pseudo-second-order kinetic: } 1/C_t = 1/C_0 + k_2 t \quad (3)$$

where C_0 is the initial dye concentration, mg/L, C_t is the concentration of dye at time t, mg/L, k_0 is the pseudo-zero-order rate constant, mg/L·min, k_1 is the pseudo-first-order rate constant, min^{-1}, k_2 is the pseudo-second-order rate constant, L/mg·min, t is the time, min.

3. Results and discussion

3.1. Surface morphology and elemental composition of ZnO and ZnO/rGO

The FESEM images of GO, ZnO and ZnO/rGO photocatalysts are shown in Figs. 1(a)–(c), respectively. The synthesized GO exhibited layered sheet-like structure as shown in Fig. 1(a). It was found that the surface of ZnO particles was smooth and the particles were uniformly distributed. In addition, the sizes of ZnO particles were found to vary from 150 to 350 nm, while the sizes of ZnO/rGO were in the range of 50–100 nm. Pure ZnO particles exhibited hexagonal crystal shapes and tend to be interconnected and agglomerated to form spherical shapes. It was anticipated that rGO sheets acted as templates and may control the particle growth during calcination which resulting in smaller size of ZnO [19]. Besides, the positively charged Zn^+ ions interacted electrostatically with the negatively charged ions via its hydrophilic functional groups such as epoxy, carboxyl and hydroxyl groups [12,20]. The large surface area and interlayer distance of rGO were highly beneficial for the effective anchoring and uniformly distribution of ZnO particles. Fig. 1(d) shows a transmission electron microscopy (TEM) image of ZnO/rGO composites. ZnO nanoparticles exhibited spherical shape, in accordance with FESEM analyses. Furthermore, it was also observed that ZnO particles were strongly anchored to rGO sheet, suggesting the successful formation of rGO–ZnO nanocomposites. It could be seen that rGO was decorated by relatively well-distributed ZnO particles rather than as separate phases of the two materials, which would be beneficial for the photocatalytic activity.

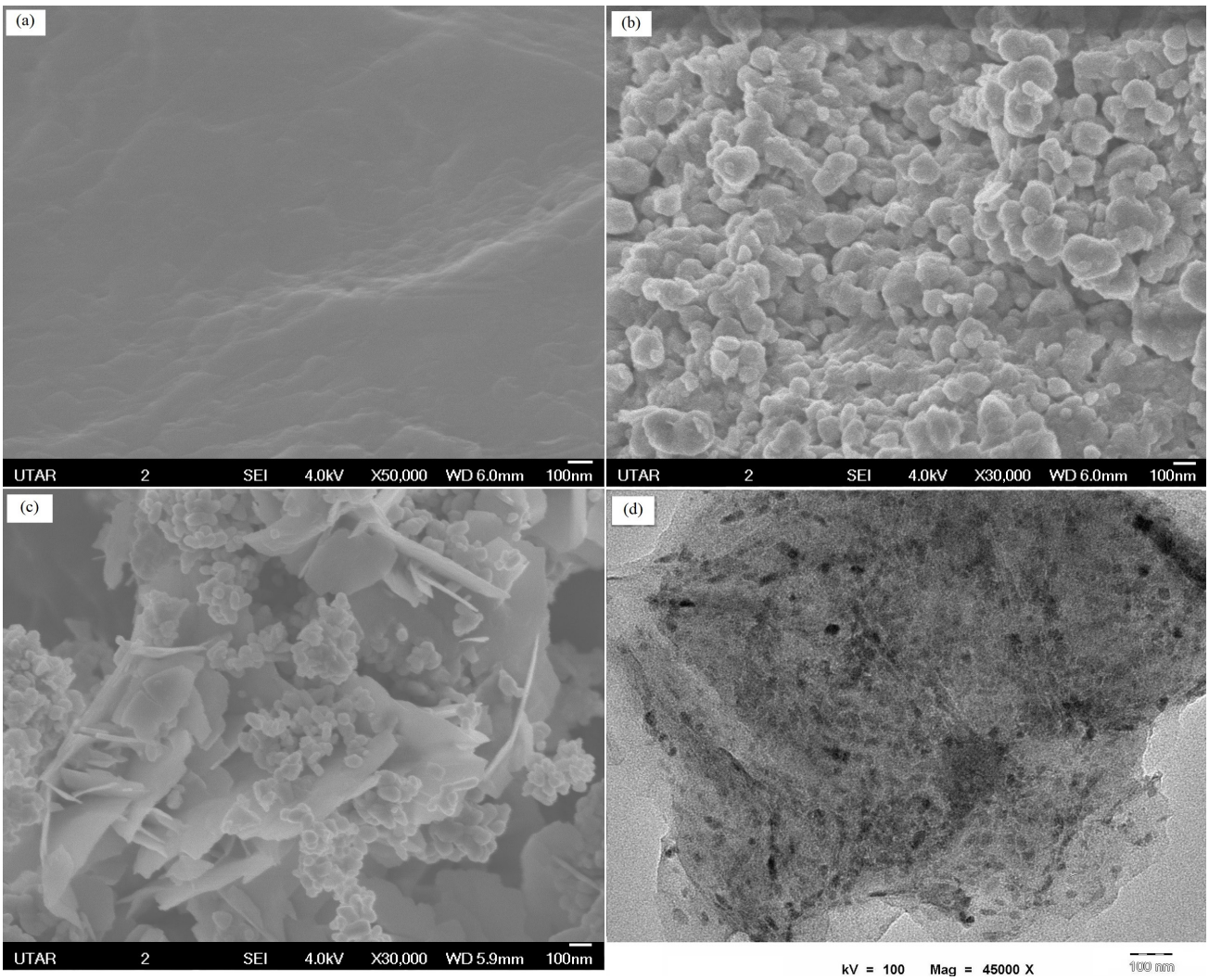

Fig. 1. FESEM images of (a) GO, (b) ZnO, (c) ZnO/rGO and (d) TEM image of ZnO/rGO.

ZnO particles might interact with rGO via carboxylic acid functional groups or simple physisorption [21]. Thus, this indicated that rGO played a pivotal role for the formation of nucleation of ZnO in ZnO/rGO photocatalysts.

Figs. 2(a) and (b) demonstrate the elemental compositions in terms of atomic percentage and weight percentage of ZnO and ZnO/rGO photocatalysts. The EDX spectrum for ZnO clearly shows that the sample was made up of Zn and O only. The relative concentration of oxygen to zinc was close to 0.63 which indicated that O element in Zn–O bonds appeared in ZnO structure was difficult to be determined by EDX analysis. Meanwhile, the EDX spectrum of ZnO/rGO proved the existence of Zn, O and C atoms. This analysis revealed that about 4.89 wt% of C element appeared in the sample ZnO/rGO. This indicated that the incorporation of ZnO into rGO through precipitation method was successfully achieved. Both spectra indicated that all the samples were free from other elemental impurities.

3.2. X-ray powder diffraction (XRD) study

Phase identification and crystallite size determination of GO, ZnO and ZnO/rGO were achieved through analysis of the XRD diffraction patterns. The diffraction patterns of GO, ZnO and ZnO/rGO are shown in Fig. 3. For pure GO, two diffraction peaks were observed at 10.8° and 43.4°, indicating complete oxidation graphite to GO [5]. The occurrence of these peaks was due to the presence of oxygen functional group in GO. The XRD patterns of the synthesized ZnO particles were in hexagonal wurtzite ZnO structure and possessed high purity. Besides, the sharp peaks of diffraction profiles also indicated that the particles were of highly crystalline phases. The peak positions of the synthesized ZnO matched well with the standard ZnO profile in which the diffraction peaks were positioned at 2θ values of 31.9°, 34.5°, 36.4°, 47,6°, 56.7°, 63.0° and 68.1° (JCPDS Card 36-1451) [22]. In addition, no characterization peaks of intermediate products such as $Zn(OH)_2$ was detected in the XRD profile.

After incorporating GO sheet with ZnO particles, the intensity of diffraction peak at 10.8° disappeared. This indicated that GO had been successfully reduced to rGO due to the loss of oxygen functional groups. The diffraction pattern of ZnO/rGO was almost similar to that of pure ZnO. No obvious diffraction peak of rGO could be observed between 20° and 29° in ZnO/rGO [23] due to its low concentration and

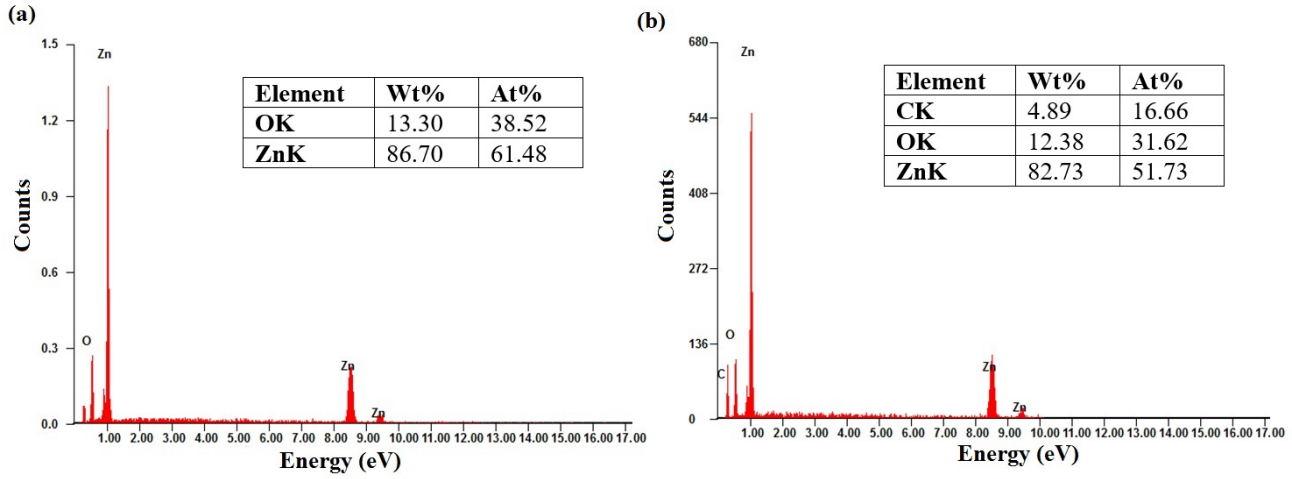

Fig. 2. EDX analysis results of (a) ZnO and (b) ZnO/rGO.

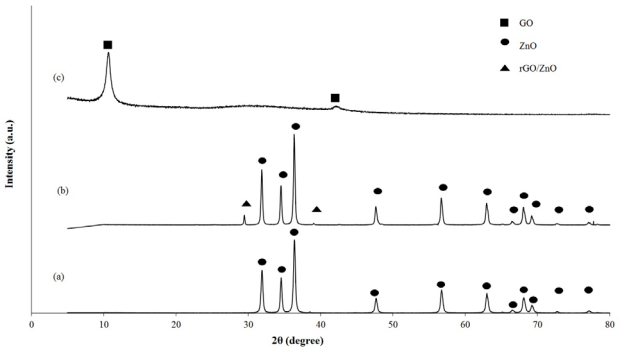

Fig. 3. XRD patterns for (a) ZnO, (b) ZnO/rGO and (c) GO.

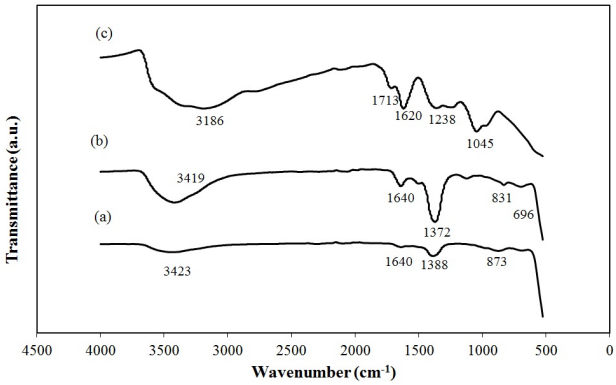

Fig. 4. FTIR spectra of (a) ZnO, (b) ZnO/rGO and (c) GO.

the extensive exfoliation of rGO. rGO can be covered considerably with ZnO particles during synthesis process. An additional small peak at 29.4° might be attributed to the complete reduction of GO to rGO via the impregnation method followed by calcination under nitrogen flow [15,24]. Besides, a small peak at 2θ of about 43.3° confirmed the preservation of graphite structure even after the reduction process [25]. In short, XRD results demonstrated that GO, ZnO and ZnO/rGO had been successfully synthesized in this study.

3.3. FTIR study

Fig. 4 illustrates the FTIR spectra of GO, ZnO and ZnO/rGO. The peaks of GO at 3,196 and 1,238 cm^{-1} were assigned to stretching and deformation of O–H. Peak of 1,238 cm^{-1} proved the existence of epoxy with C–O stretching while peaks of 1,713 and 1,045 cm^{-1} showed the presence of carbonyl and carboxylic acid with C=O and C–O (alkoxy) stretching vibration in GO [26,27]. The band at 1,620 cm^{-1} was attributed to the vibration of water molecules and skeletal vibrations of unoxidized graphitic domains [27]. While most of the functional groups remained in the composites, a new adsorption band was observed around 1,500 cm^{-1} in ZnO/rGO which attributed to the C=C skeletal vibration of rGO [26,28]. Meanwhile, recent studies showed that Raman spectroscopy peaks at 1,570 and 2,700 cm^{-1} confirmed the G and D bands for both GO and rGO catalysts [18]. This suggested the sp^2 hybridization of graphitic carbon and carbon lattice distortion.

Both ZnO and ZnO/rGO have five similar peaks as shown in Fig. 4. First, the broad peaks at 3,432 and 3,419 cm^{-1} are attributed to the O–H stretching vibration mode of the hydroxyl group from water molecules that were adsorbed on the catalysts surface [29]. Meanwhile, the absorption bands at around ~1,640 and 1,370–1,380 cm^{-1} correspond to the C–H bonding and O–H deformations of C–OH groups, respectively [30,31]. The weak peaks at 873 and 831 cm^{-1} for ZnO and ZnO/rGO, respectively, are assigned to the C–H group. Lastly, the characteristic peak at around 500–600 cm^{-1} corresponds to the Zn–O bonding which confirms the successful synthesis of ZnO particles [7].

It is evident that ZnO/rGO possesses new weak peaks at 1,502 and 1,124 cm^{-1}. These peaks are assigned to the skeletal vibration of the graphene sheets and stretching vibration of aromatic C=C, respectively [8,15]. In addition, the FTIR spectrum of ZnO/rGO shows no peaks at 1,726, 1,625, 1,225, 1,077 and 1,052 cm^{-1} which correspond to C=O of COOH group, sp^2 hybridized C–C group, phenolic C–O–H group, epoxy symmetrical ring C–O–C group and C–O group, respectively [7,15,31]. The disappearance of the said peaks indicated that the oxygen-containing groups in GO were completely

removed and GO was converted to rGO [20,23]. The synthesized ZnO/rGO material with enormous number of electroactive sites could exhibit excellent adsorption capacity followed by photocatalytic activity for the degradation of various organic dyes.

3.4. Degradation of various organic dyes

The degradation of various organic dyes, that is, methyl orange, congo red and rhodamine B, using synthesized photocatalysts was investigated. Figs. 5(a) and (b) depict the degradation efficiencies of various organic dyes using ZnO and ZnO/rGO, respectively. Photocatalytic degradation efficiencies of organic dyes in the presence of ZnO/rGO (40.94%, 57.62% and 97.52% for methyl orange, rhodamine B and congo red, respectively) were significantly higher than those of ZnO (4.87%, 20.96% and 22.98% for methyl orange, rhodamine B and congo red, respectively). It is noteworthy that SEM and XRD analyses have suggested that the particles and crystallite sizes of ZnO were larger than those of ZnO/rGO and theoretically, smaller sizes should demonstrate better performance. High surface area to volume ratio is generally beneficial for the absorption of photons and light [7]. Thus, it was found that the catalytic activity of the synthesized ZnO/rGO was higher than that of ZnO in this study.

Azarang et al. [7] reported that introducing ZnO into rGO would increase the surface electric charge of the photocatalyst, which consequently increased its absorbance due to the attractive force acting between rGO and ZnO. It had been reported that rGO was a good electron acceptor and semiconductor ZnO was a good electron donor [5,9]. rGO would receive photogenerated electrons which promote interfacial electron transfer from the adhered ZnO for the subsequent redox reaction on the photocatalyst surface. In other words, the photocatalytic degradation of organic dyes could be enhanced due to the suppressed recombination rate of photogenerated electron–hole pairs. Besides, graphene-based materials exhibit advanced features such as high adsorption of organic dyes and strong π–π stacking with dye chromophores [19]. Hence, ZnO/rGO which possessed excellent degradation efficiency was chosen as photocatalysts for subsequent studies.

Photocatalytic degradation efficiency of congo red in the presence of ZnO with 1, 3, 5 and 10 wt% ZnO/rGO were recorded at 22.98%, 45.62%, 78.13%, 97.52% and 90.67%, respectively. The photocatalytic performance decreased when excessive amount of rGO content was added. Zhang et al. [32] reported that excessive amount of rGO content would create light harvesting competition between ZnO and rGO because rGO could act as charge carrier recombination centre to promote the recombination of electron–hole pairs in rGO. They found that the weight addition ratio of GO into the semiconductor matrix was generally not more than 5%. Thus, 5 wt% of GO in the ZnO/rGO composite was selected as the optimum to be further studied in this study.

Besides, the photocatalytic degradation efficiency of organic dyes using both catalysts showed a clear trend where congo red > rhodamine B > methyl orange. It was reported that methyl orange was more challenging to be degraded due to the $-SO_3^-$ groups which were attached to the surface of photocatalyst through two sulphonic oxygen could form a strong covalent bond [33]. Therefore, the number of active sites available would decrease since the dye molecules adsorbed on the surface were not easily detached after the oxidation reaction. Meanwhile, rhodamine B was reported to possess high resistance towards photodegradation due to its ammonium and oxinium structure [34,35]. It was suggested that high degradation efficiency of congo red was due to the rapid reaction occurred with the cleavage of azo bond (–N=N–) [36]. Hence, the conjugated system of congo red easily broken down resulting in higher degradation efficiency. Besides, the generated hydroxyl radicals would attack and destroy the aromatic rings to form smaller organic compounds [4]. Moreover, the hydroxyl radicals also attacked N=N bond leading to the rapid disappearance of the colour. Adsorption efficiencies for congo red in the presence of ZnO and ZnO/rGO photocatalysts were 7.19% and 20.68%, respectively. This indicated that adsorption process did not contribute much to the photocatalytic degradation efficiency. Therefore, congo red with the highest photocatalytic degradation efficiency was chosen as the model pollutant for subsequent studies.

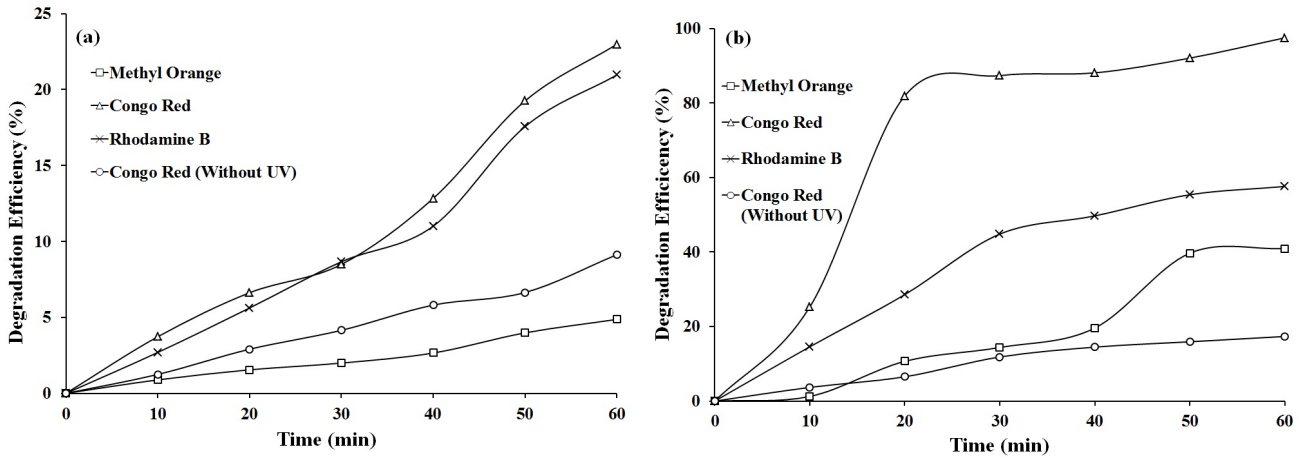

Fig. 5. Effect of various organic dyes on the photocatalytic degradation by (a) ZnO and (b) ZnO/rGO photocatalysts (catalyst dosage = 2 g/L, initial dye concentration = 10 mg/L, reaction time = 1 h, initial pH = 7).

3.5. Effect of initial dye concentration

The effect of initial dye concentrations (10, 20, 30, 40 and 50 mg/L) was investigated by measuring the photodegradation efficiency in the presence of ZnO/rGO. Fig. 6 shows that as the dye concentration increased from 10 to 50 mg/L, the degradation efficiency decreased from 97.52% to 48.62%. Increasing dye concentration would stimulate the competition between the dye and intermediate molecules for the adsorption to undergo photocatalysis reaction at a later stage [37]. Besides, as the colour of dye solution became darker, the amount of photons absorbed by the ZnO/rGO could reduce due to the poor penetration of light [38]. Moreover, high concentration also resulted in the aggregation of dye molecules, which could aggravate the hydrophobic interactions between aromatic rings and consequently affect the degradation rate [39]. As a result, increasing the amount of dye molecules adsorbed and reacted on the photocatalyst's surface would result in the reduction of the accessible active sites. Hence, the generated hydroxyl radicals adsorbed on the surface of photocatalyst would reduce as the active sites were occupied by dye molecules. The optimal condition of 10 mg/L congo red solution with the highest degradation efficiency was chosen for subsequent studies.

3.6. Effect of catalyst dosage

The effect of catalyst dosage (0, 0.5, 1.0, 1.5, 2.0 and 2.5 g/L) in the photocatalytic degradation of congo red using ZnO/rGO was then investigated. It can be observed that as the ZnO/rGO dosage increased from 0 to 2.0 g/L, the degradation efficiency increased significantly from 8.90% to 97.52% as shown in Fig. 7. The poor performance for dosage below 2 g/L could be explained by the limited active sites available for the reaction [40]. Hence, the generation of hydroxyl radicals could be enhanced with increasing catalyst loading and more dye molecules could be adsorbed to react on the surface of ZnO/rGO. However, with further increment in the catalyst dosage beyond 2 g/L, the degradation efficiency slightly reduced from 97.52% to 87.37%. The increment in the turbidity caused by the particles would hinder light penetration pathway [37]. Therefore, it would result in the increment of light scattering effect as well as aggregation of particles. In other words, the photocatalytic degradation efficiency would decrease as the generation of radicals reduced. Thus, 2.0 g/L of ZnO/rGO dosage with the highest degradation efficiency was identified to be the optimum condition for the subsequent study on photocatalytic degradation of congo red.

3.7. Effect of solution pH

Photocatalytic degradation efficiency of congo red was then investigated by varying the pH value of the solutions (pH 3, 5, 7, 9 and 11). The results clearly demonstrated that pH 5 and pH 7 achieved the highest photocatalytic degradation of congo red which were about 97.52% and 97.96%, respectively (Fig. 8). As the solution pH was increased from 3 to 7, the degradation efficiency increased from 66.49% to 97.96%. However, there was a decrement in the photocatalytic degradation efficiency from 97.96% to 81.35% when the solution pH was further increased from 7 to 11. It was reported that the effect of pH solution on the photocatalytic degradation was related to the acidity of photocatalyst and dye. Besides, zero point charge of metal oxide could also be

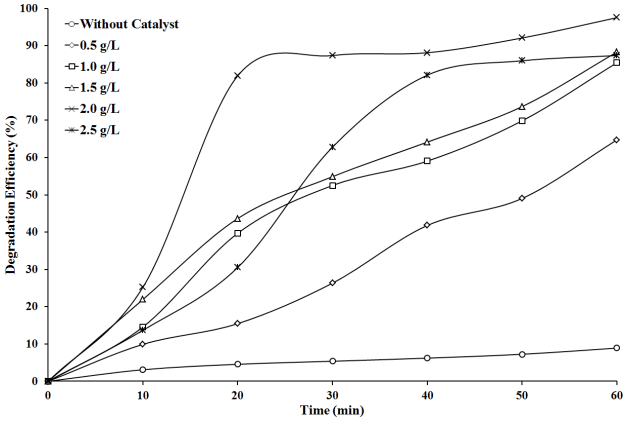

Fig. 7. Effect of catalyst dosage on the photocatalytic degradation by ZnO/rGO photocatalyst (initial congo red concentration = 10 mg/L, reaction time = 1 h, initial pH = 5).

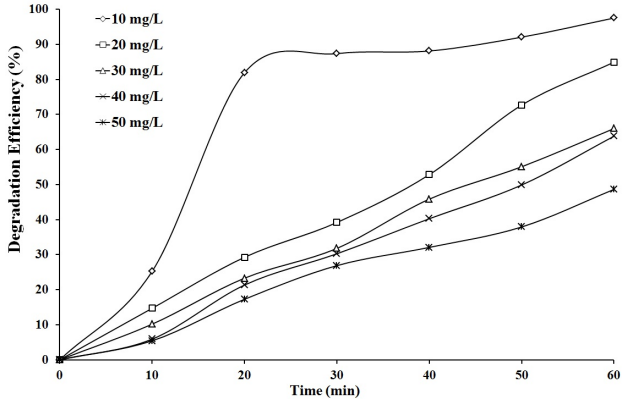

Fig. 6. Effect of initial congo red concentration on the photocatalytic degradation by ZnO/rGO photocatalyst (ZnO/rGO dosage = 2 g/L, reaction time = 1 h, initial pH = 5).

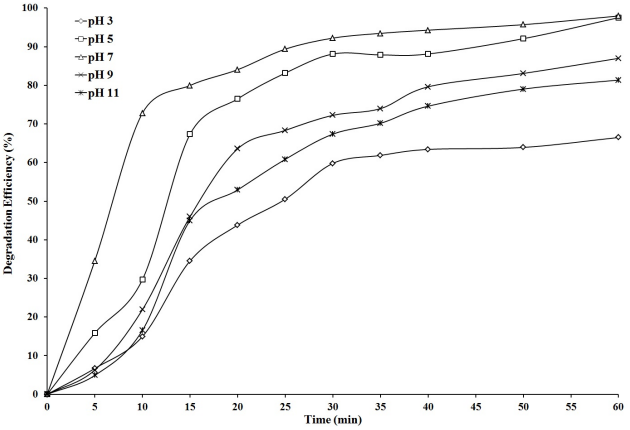

Fig. 8. Effect of solution pH on the photocatalytic degradation by ZnO/rGO photocatalyst (ZnO/rGO dosage = 2 g/L, initial congo red concentration = 10 mg/L, reaction time = 1 h).

correlated to the photocatalytic degradation efficiency. It had been reported that congo red is an anionic dye while ZnO had zero point charge at pH 9 [41]. This indicated that below pH 9, the surface of photocatalyst was positively charged, but it was negatively charged above pH 9. Below the zero point charge, the surface of the photocatalyst was covered by H^+ ions, while above the zero point charge; it was covered by OH^-. At solution pH 3, excess amount of H^+ would interact with azo bond (–N=N–) and hence the electron densities at azo group decreased [38]. In other words, the reactivity of hydroxyl radicals at low pH decreased. Hence, the dye molecules adsorbed on the surface of ZnO/rGO also reduced. Below zero point charge (pH 5 and 7), the electrostatic attraction between the positively charged ZnO/rGO and negatively charged congo red would enhance the adsorption of dye molecules on ZnO/rGO, thereby, increasing the formation of reactive free radicals. Theoretically, dye adsorption on the adsorbent surface played an essential role during photocatalytic degradation process as higher adsorption should enhance the degradation efficiency [42]. Conversely, the surface of ZnO/rGO was negatively charged at pH 9 and pH 11 as it was covered by OH^-. Thus, there was electrostatic repulsion between negatively charged ZnO/rGO and negatively charged congo red. This would result in the decrement of degradation efficiency at alkaline solution. Therefore, the solution pH of 7 with the highest degradation efficiency was chosen for the reusability and kinetic studies.

3.8. Reusability study

As depicted in Fig. 9, the degradation efficiencies for fresh ZnO/rGO and spent ZnO/rGO were 97.96% and 96.67%, respectively. It was noted that the spent ZnO/rGO still exhibited high photocatalytic performance and hence ZnO/rGO was reusable. Besides, this indicated that ZnO/rGO possessed good stability in the reaction. The slightly decrement in the degradation performance of spent ZnO/rGO material might be related to the appearance of oxygen-containing groups in rGO and caused the reduction of electron mobility. It was reported that the degradation efficiency of 10 mg/L methyl orange in the presence of 0.25 g/L ZnO under sunlight for a duration of 2 h was reduced from 53% to 20% after four catalytic uses [43]. In addition, it was claimed that 0.5 g/L of ZnO degraded 5 mg/L of methylene blue under sunlight for a duration of 2 h and suffered 3.2% and 9.4% of losses after two and four catalytic cycles, respectively [24]. In this study, photocatalytic degradation efficiency of congo red in the presence of reused ZnO/rGO marginally decreased by 1.29% only. Hence, it was concluded that ZnO/rGO was recyclable and indeed a promising photocatalyst for photocatalytic degradation of organic dyes in water.

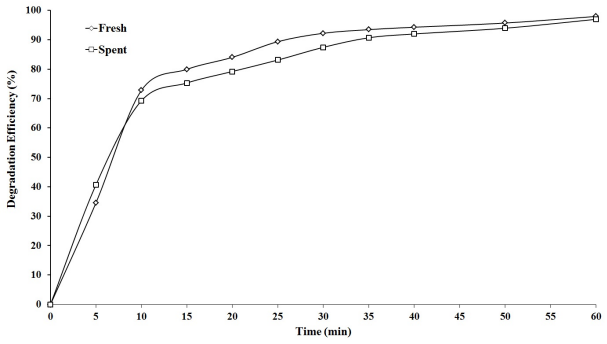

Fig. 9. Degradation of congo red in the presence of fresh and spent ZnO/rGO photocatalyst (ZnO/rGO dosage = 2 g/L, initial congo red concentration = 10 mg/L, reaction time = 1 h, initial pH = 7).

3.9. Kinetic study

The kinetic study was performed based on the disappearance of congo red dye at an initial concentration of 10 mg/L but with different solution pH values. In order to determine the reaction order of the photocatalytic degradation by ZnO/rGO, pseudo-zero-order, pseudo-first-order and pseudo-second-order graphs are plotted (Fig. 10). Table 1 tabulates the reaction rate constants for degradation of congo red under different pH values. Fig. 10(b) shows the graph of $\ln(C_0/C_t)$ vs. time t. It was observed that the photocatalytic degradation of congo red satisfactorily fitted a pseudo-first-order kinetic as the coefficient of determination (R^2) is close to 1. Hence, it was suggested that the gradient of the best fit line should be based on the pseudo-first-order rate constant. It was noted that the rate constant significantly increases from 0.0285 to 0.0917 min^{-1} as the solution pH was increased from 3 to 7. It was worth highlighting that the current finding was significantly higher than the results obtained by Zhao et al. [11] where the optimum photocatalytic activity with an apparent rate constant of 0.025 min^{-1} was exhibited by ZnO/rGO composites with a moderate ZnO content of 29.53 wt%. However, further increasing the solution pH to 9 and 11, the reaction rate constants significantly decreased to 0.0437 and 0.0365 min^{-1}, respectively. The decreasing trend had been explained in section 3.7.

3.10. COD removal

Sample of congo red solution obtained after photocatalytic degradation under optimized conditions, that is, ZnO/rGO dosage of 2 g/L, congo red concentration of 10 mg/L and at pH 7 was collected to study the COD removal. It was noted that the COD values of the solution before and after the photocatalytic degradation were 64 and 0 mg/L, respectively. From the result, it could be concluded that 100% of COD reduction was achieved after 1 h. At the end of the photocatalytic reaction, the colour of degraded congo red solution completely changed from red colour to colourless solution. As 100% of COD removal was achieved, it was suggested that complete oxidation of the dye was achieved. This result suggested that ZnO/rGO composite was a high potential photocatalyst for the degradation of congo red leading to its mineralization.

3.11. Proposed reaction mechanism

Photocatalytic reactions usually consist of four steps: (1) absorption of photons by the photocatalysts; (2) creation of photoexcited hole–electron pairs; (3) hole–electron pairs separation and migration to photocatalysts surface and (4) redox reaction on the photocatalyst surface [5]. Fig. 11 shows the proposed mechanism of heterogeneous photocatalytic process when the reactants are adsorbed and reacted on the

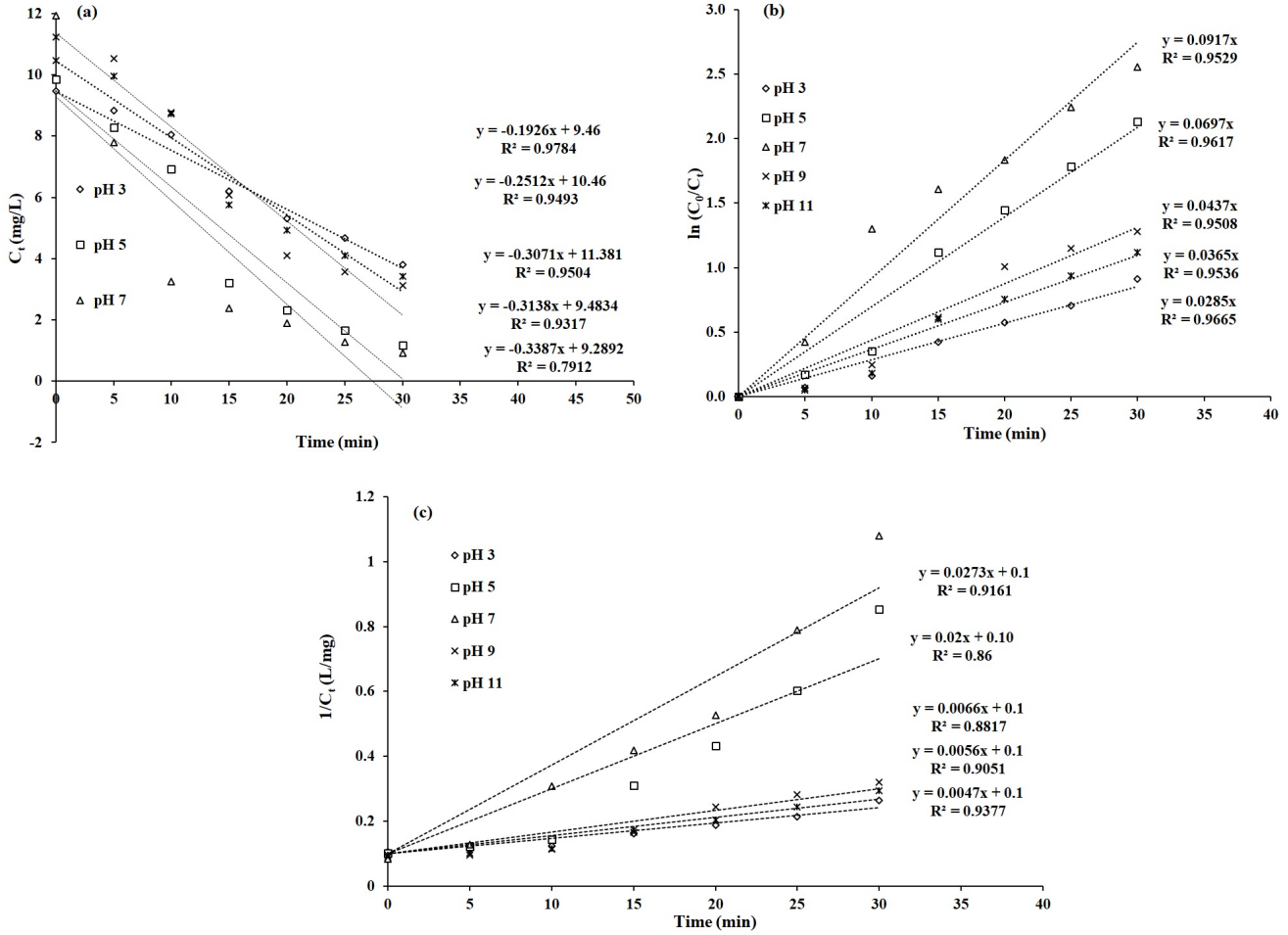

Fig. 10. Reaction kinetic plots for photocatalytic degradation of congo red: (a) pseudo-zero-order, (b) pseudo-first-order, (c) pseudo-second-order (ZnO/rGO dosage = 2 g/L, initial congo red concentration = 10 mg/L, reaction time = 1 h).

Table 1
Reaction rates and coefficient of determinations for photocatalytic degradation of congo red at various solution pH for pseudo-zero-order, pseudo-first-order and pseudo-second-order reactions

pH	Pseudo-zero-order model		Pseudo-first-order model		Pseudo-second-order model	
	R^2	k_1 (mg/L·min)	R^2	k_2 (min^{-1})	R^2	k_3 (L/mg·min)
3	0.9784	0.1926	0.9665	0.0285	0.1279	0.0093
5	0.9278	0.3307	0.9617	0.0697	0.9141	0.0246
7	0.6432	0.4606	0.9529	0.0917	0.9489	0.0319
9	0.9498	0.3007	0.9508	0.0437	0.8125	0.0113
11	0.9493	0.2512	0.9536	0.0365	0.6435	0.0102

surface of the semiconductor catalyst. To undergo the degradation process, photocatalytic reaction was initiated by the absorption of UV radiation at wavelengths exceeding the ZnO's band-gap energy of 3.2 eV (i.e., <387 nm) [7,8]. The CB and VB for ZnO were −4.05 and −7.25 eV (vs. vacuum), respectively, and the work function of rGO was −4.8 eV [7]. Under UV radiation, the electrons were excited from VB to CB and holes were generated in VB (Eq. (4)). The generated electrons by ZnO CB would 'hop' to rGO as the energy for CB of ZnO was more positive than that of rGO (Eq. (5))]. These electrons would then transfer to C2p orbitals of graphene due to the electrostatic force and led to hole–electron separation. This was ascribed to the 2D π-conjugation structure of rGO and acted as an excellent electron-accepting and transport material. The holes can either react with water or with the surface hydroxyl ions on the ZnO to produce hydroxyl radicals (Eqs. (6) and (7)) [4]. Meanwhile, electron plays a vital role to reduce oxygen molecules to produce superoxide ions effectively (Eq. (8)). Lastly, the dyes can be degraded by the generated holes, superoxide ions and hydroxyl radicals.

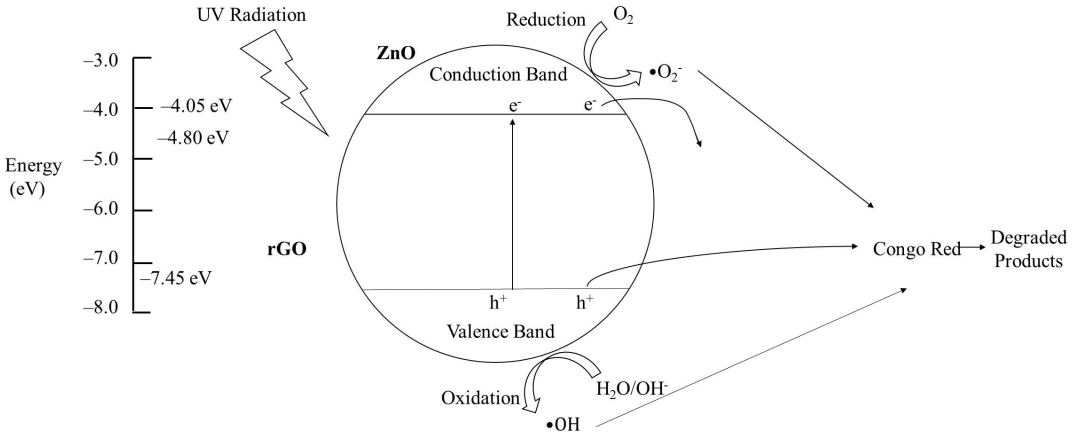

Fig. 11. Proposed mechanism of photocatalytic degradation of congo red by ZnO/rGO.

$$ZnO + hv \rightarrow ZnO\ (e^- + h^+) \quad (4)$$

$$e^- + rGO \rightarrow rGO\ (e^-) \quad (5)$$

$$h^+ + H_2O \rightarrow H^+ + {}^\bullet OH \quad (6)$$

$$h^+ + OH^- \rightarrow {}^\bullet OH \quad (7)$$

$$rGO\ (e^-) + O_2 \rightarrow rGO + {}^\bullet O_2^- \quad (8)$$

It was noted that no optical properties tests (photoluminescence or photoelectrochemical analysis) were conducted in this study as the scope was only to study the degradation efficiency rather than the changes on electronic and optical properties of the ZnO/rGO and charge carriers separation and transfer. However, Zhang et al. [32,44,45] research groups had verified that the coupling of appropriate amount rGO with various kind of semiconductors could significantly inhibited the recombination of the photogenerated electron–hole pairs over rGO/semiconductor via photoluminescence and electrochemical impedance analyses. This optimized the charge carrier transfer pathway across the interface between semiconductor and rGO, thus, prolong the lifetime of photogenerated charge carriers.

4. Conclusions

Photocatalysts, ZnO and ZnO/rGO were successfully synthesized using the impregnation method and characterized by different techniques such as field emission scanning microscopy-energy dispersive X-ray analysis (FESEM-EDX) and XRD and FTIR. FESEM analyses showed that the particles of both photocatalysts were of spherical shape while EDX analyses indicated that the samples were free from other elemental impurities. In addition, additional peaks found in XRD and FTIR results confirmed that rGO was successfully introduced into ZnO. Besides, the highest photocatalytic degradation of congo red (97.96%) was achieved in the presence of ZnO/rGO in 1 h under the optimal conditions (10 mg/L congo red, 2.0 g/L ZnO/rGO and solution pH 7). It was worth noting that 100% removal of COD could be achieved after 1 h of photocatalytic degradation of congo red in the presence of ZnO/rGO. In addition, the spent ZnO/rGO still exhibited high photocatalytic performance of 96.67%. In kinetic study, the pseudo-first-order kinetic reaction was applicable to the photocatalytic degradation process of congo red. The pseudo-first-order reaction rate constant for ZnO/rGO under the optimal conditions was 0.0917 min^{-1}. Therefore, it was deduced that the photocatalytic degradation of congo red in the presence of ZnO/rGO could be efficiently performed as a promising means to degrade organic dyes in wastewater.

Acknowledgements

This study was financially supported by Universiti Tunku Abdul Rahman Research Grant through the Centre for Photonics and Advanced Materials Research and Centre for Environment and Green Technology (CEGT), UTAR. The financial support provided by Fundamental Research Grant Scheme by the Ministry of Education (MOE) Malaysia is also gratefully acknowledged.

References

[1] H. Fida, G. Zhang, S. Guo, A. Naeem, Heterogeneous Fenton degradation of organic dyes in batch and fixed bed using La-Fe montmorillonite as catalyst, J. Colloid Interface Sci., 490 (2017) 859–868.
[2] S.K. Sen, S. Raut, P. Bandyopadhyay, S. Raut, Fungal decolouration and degradation of azo dyes: a review, Fungal Biol. Rev., 30 (2016) 112–133.
[3] G. Jenita Rani, M.A. Jothi Rajan, G. Gnana Kumar, Reduced graphene oxide/$ZnFe_2O_4$ nanocomposite as an efficient catalyst for the photocatalytic degradation of methylene blue dye, Res. Chem. Intermed., 43 (2017) 2669–2690.
[4] M. Cheng, G. Zeng, D. Huang, C. Lai, P. Xu, C. Zhang, Y. Liu, Hydroxyl radicals based advanced oxidation processes (AOPs) for remediation of soils contaminated with organic compounds: a review, Chem. Eng. J., 284 (2016) 582–598.
[5] P. Wang, S. Zhan, Y. Xia, S. Ma, Q. Zhou, Y. Li, The fundamental role and mechanism of reduced graphene oxide in rGO/Pt-TiO_2 nanocomposite for high-performance photocatalytic water splitting, Appl. Catal., B, 207 (2017) 335–346.
[6] C.B. Ong, A.W. Mohammad, L.Y. Ng, E. Mahmoudi, S. Azizkhani, N.H. Hayati Hairom, Solar photocatalytic and surface enhancement of ZnO/rGO nanocomposite: degradation of perfluorooctanoic acid and dye, Process Saf. Environ. Prot., 112 (2017) 298–307.
[7] M. Azarang, A. Shuhaimi, R. Yousefi, S.P. Jahromi, One-pot sol–gel synthesis of reduced graphene oxide uniformly decorated zinc oxide nanoparticles in starch environment for highly

efficient photodegradation of Methylene Blue, RSC Adv., 5 (2015) 21888–21896.
[8] S.Y. Sawant, M.H. Cho, Facile electrochemical assisted synthesis of ZnO/graphene nanosheets with enhanced photocatalytic activity, RSC Adv., 5 (2015) 97788–97797.
[9] Y.-C. Pu, H.-Y. Chou, W.-S. Kuo, K.-H. Wei, Y.-J. Hsu, Interfacial charge carrier dynamics of cuprous oxide-reduced graphene oxide (Cu_2O-rGO) nanoheterostructures and their related visible-light-driven photocatalysis, Appl. Catal., B, 204 (2017) 21–32.
[10] W. Yang, C. Li, L. Wang, S. Sun, X. Yan, Solvothermal fabrication of activated semi-coke supported TiO_2-rGO nanocomposite photocatalysts and application for NO removal under visible light, Appl. Surf. Sci., 353 (2015) 307–316.
[11] Y. Zhao, L. Liu, T. Cui, G. Tong, W. Wu, Enhanced photocatalytic properties of ZnO/reduced graphene oxide sheets (rGO) composites with controllable morphology and composition, Appl. Surf. Sci., 412 (2017) 58–68.
[12] J. Salamon, Y. Sathishkumar, K. Ramachandran, Y.S. Lee, D.J. Yoo, A.R. Kim, G. Gnana kumar, One-pot synthesis of magnetite nanorods/graphene composites and its catalytic activity toward electrochemical detection of dopamine, Biosens. Bioelectron., 64 (2015) 269–276.
[13] N. Zhang, M.Q. Yang, S. Liu, Y. Sun, Y.J. Xu, Waltzing with the versatile platform of graphene to synthesize composite photocatalysts, Chem. Rev., 115 (2015) 10307–10377.
[14] F.T. Johra, W.-G. Jung, RGO–TiO_2–ZnO composites: synthesis, characterization, and application to photocatalysis, Appl. Catal., A, 491 (2015) 52–57.
[15] W. Kang, X. Jimeng, W. Xitao, The effects of ZnO morphology on photocatalytic efficiency of ZnO/RGO nanocomposites, Appl. Surf. Sci., 360 (2016) 270–275.
[16] N. Kumar, A.K. Srivastava, H.S. Patel, B.K. Gupta, G.D. Varma, Facile synthesis of ZnO-reduced graphene oxide nanocomposites for NO_2 gas sensing applications, Eur. J. Inorg. Chem., 2015 (2015) 1912–1923.
[17] E. Mahmoudi, L.Y. Ng, M.M. Ba-Abbad, A.W. Mohammad, Novel nanohybrid polysulfone membrane embedded with silver nanoparticles on graphene oxide nanoplates, Chem. Eng. J., 277 (2015) 1–10.
[18] N.K. Zaman, R. Rohani, A.W. Mohammad, A.M. Isloor, Polyimide-graphene oxide nanofiltration membrane: characterizations and application in enhanced high concentration salt removal, Chem. Eng. Sci., 177 (2018) 218–233.
[19] M. Huang, J. Yu, Q. Hu, W. Su, M. Fan, B. Li, L. Dong, Preparation and enhanced photocatalytic activity of carbon nitride/titania (001 vs 101 facets)/reduced graphene oxide (g-C_3N_4/TiO_2/rGO) hybrids under visible light, Appl. Surf. Sci., 389 (2016) 1084–1093.
[20] M. Vinothkannan, C. Karthikeyan, G. Gnana Kumar, A.R. Kim, D.J. Yoo, One-pot green synthesis of reduced graphene oxide (RGO)/Fe_3O_4 nanocomposites and its catalytic activity toward methylene blue dye degradation, Spectrochim. Acta, Part A, 136 (2015) 256–264.
[21] H. Wu, S. Lin, C. Chen, W. Liang, X. Liu, H. Yang, A new ZnO/rGO/polyaniline ternary nanocomposite as photocatalyst with improved photocatalytic activity, Mater. Res. Bull., 83 (2016) 434–441.
[22] S. Xu, L. Fu, T.S.H. Pham, A. Yu, F. Han, L. Chen, Preparation of ZnO flower/reduced graphene oxide composite with enhanced photocatalytic performance under sunlight, Ceram. Int., 41 (2015) 4007–4013.
[23] G. Gnana Kumar, K. Justice Babu, K.S. Nahm, Y.J. Hwang, A facile one-pot green synthesis of reduced graphene oxide and its composites for non-enzymatic hydrogen peroxide sensor applications, RSC Adv., 4 (2014) 7944–7951.
[24] F.S. Omar, H. Nay Ming, S.M. Hafiz, L.H. Ngee, Microwave synthesis of zinc oxide/reduced graphene oxide hybrid for adsorption-photocatalysis application, Int. J. Photoenergy, 2014 (2014) 1–8.
[25] V. Kavimani, P.K. Soorya, R. Rajesh, D. Rammasamy, N.B. Selvaraj, T. Yang, B. Prabakaran, S. Jothi, Electrodeposition of r-GO/SiC nano-composites on magnesium and its corrosion behavior in aqueous electrolyte, Appl. Surf. Sci., 424 (2017) 63–71.
[26] J. Hu, H. Li, Q. Wu, Y. Zhao, Q. Jiao, Synthesis of TiO_2 nanowire/reduced graphene oxide nanocomposites and their photocatalytic performances, Chem. Eng. J., 263 (2015) 144–150.
[27] Y. Wang, J. Liu, L. Liu, D.D. Sun, High-quality reduced graphene oxide-nanocrystalline platinum hybrid materials prepared by simultaneous co-reduction of graphene oxide and chloroplatinic acid, Nanoscale Res. Lett., 6 (2011) 241.
[28] P. Sun, H. Liu, K. Wang, M. Zhong, D. Wu, H. Zhu, Selective ion transport through functionalized graphene membranes based on delicate ion–graphene interactions, J. Phys. Chem. C, 118 (2014) 19396–19401.
[29] B. Bhuyan, B. Paul, D.D. Purkayastha, S.S. Dhar, S. Behera, Facile synthesis and characterization of zinc oxide nanoparticles and studies of their catalytic activity towards ultrasound-assisted degradation of metronidazole, Mater. Lett., 168 (2016) 158–162.
[30] C. Zhang, J. Zhang, Y. Su, M. Xu, Z. Yang, Y. Zhang, ZnO nanowire/reduced graphene oxide nanocomposites for significantly enhanced photocatalytic degradation of Rhodamine 6G, Physica E, 56 (2014) 251–255.
[31] Y. Peng, J. Ji, D. Chen, Ultrasound assisted synthesis of ZnO/reduced graphene oxide composites with enhanced photocatalytic activity and anti-photocorrosion, Appl. Surf. Sci., 356 (2015) 762–768.
[32] N. Zhang, M.Q. Yang, Z.R. Tang, Y.J. Xu, Toward improving the graphene-semiconductor composite photoactivity via the addition of metal ions as generic interfacial mediator, ACS Nano, 8 (2014) 623–633.
[33] A.A. Khataee, M.B. Kasiri, Photocatalytic degradation of organic dyes in the presence of nanostructured titanium dioxide: influence of the chemical structure of dyes, J. Mol. Catal. A: Chem., 328 (2010) 8–26.
[34] X.X. Xue, K. Hanna, N. Deng, Fenton-like oxidation of Rhodamine B in the presence of two types of iron (II, III) oxide, J. Hazard. Mater., 166 (2009) 407–414.
[35] A.K. Mittal, C. Venkobachar, Uptake of cationic dyes by sulfonated coal: sorption mechanism, Ind. Eng. Chem. Res., 35 (1996) 1472–1474.
[36] M. Rauf, S.S. Ashraf, Radiation induced degradation of dyes—an overview, J. Hazard. Mater., 166 (2009) 6–16.
[37] M. Golshan, M. Zare, G. Goudarzi, M. Abtahi, A.A. Babaei, Fe_3O_4@HAP-enhanced photocatalytic degradation of Acid Red 73 in aqueous suspension: optimization, kinetic, and mechanism studies, Mater. Res. Bull., 91 (2017) 59–67.
[38] T.K. Roy, N.K. Mondal, Photocatalytic degradation of congo red dye on thermally activated zinc oxide, Int. J. Sci. Res. Environ. Sci., 2 (2014) 457–469.
[39] M. Rochkind, S. Pasternak, Y. Paz, Using dyes for evaluating photocatalytic properties: a critical review, Molecules, 20 (2014) 88–110.
[40] A. Elaziouti, B. Ahmed, ZnO-assisted photocatalytic degradation of congo red and benzopurpurine 4B in aqueous solution, J. Chem. Eng. Process Technol., 2 (2011) 1–9.
[41] G. Boczkaj, A. Fernandes, Wastewater treatment by means of advanced oxidation processes at basic pH conditions: a review, Chem. Eng. J., 320 (2017) 608–633.
[42] H.P. Jing, C.C. Wang, Y.W. Zhang, P. Wang, R. Li, Photocatalytic degradation of methylene blue in ZIF-8, RSC Adv., 4 (2014) 54454–54462.
[43] R. Kitture, S.J. Koppikar, R. Kaul-Ghanekar, S. Kale, Catalyst efficiency, photostability and reusability study of ZnO nanoparticles in visible light for dye degradation, J. Phys. Chem. Solids, 72 (2011) 60–66.
[44] N. Zhang, S. Xie, B. Weng, Y.J. Xu, Vertically aligned ZnO-Au@CdS core-shell nanorod arrays as an all-solid-state vectorial Z-scheme system for photocatalytic application, J. Mater. Chem. A, 4 (2016) 18804–18814.
[45] M.Q. Yang, C. Han, N. Zhang, Y.J. Xu, Precursor chemistry matters in boosting photoredox activity of graphene/semiconductor composites, Nanoscale, 7 (2015) 18062–18070.